^{6}Li in metal-poor halo stars: real or spurious?

M. Steffen[1], R. Cayrel[2], P. Bonifacio[2,3,4], H.-G. Ludwig[2,3], E. Caffau[2]

[1]Astrophysikalisches Institut Potsdam, Potsdam, Germany

[2]GEPI, Observatoire de Paris/Meudon, France

[3]CIFIST Marie Curie Excellence Team, Observatoire de Paris/Meudon, France

[4]INAF, Observatorio Astronomico di Trieste, Trieste, Italy

Abstract. The presence of convective motions in the atmospheres of metal-poor halo stars leads to systematic asymmetries of the emergent spectral line profiles. Since such line asymmetries are very small, they can be safely ignored for standard spectroscopic abundance analysis. However, when it comes to the determination of the ^{6}Li/^{7}Li isotopic ratio, $q(\mathrm{Li})=n(^6\mathrm{Li})/n(^7\mathrm{Li})$, the intrinsic asymmetry of the ^{7}Li line must be taken into account, because its signature is essentially indistinguishable from the presence of a weak ^{6}Li blend in the red wing of the ^{7}Li line. In this contribution we quantity the error of the inferred ^{6}Li/^{7}Li isotopic ratio that arises if the convective line asymmetry is ignored in the fitting of the $\lambda\,6707$ Å lithium blend. Our conclusion is that ^{6}Li/^{7}Li ratios derived by Asplund *et al.* (2006), using symmetric line profiles, must be reduced by typically $\Delta q(\mathrm{Li}) \approx 0.015$. This diminishes the number of certain ^{6}Li detections from 9 to 4 stars or less, casting some doubt on the existence of a ^{6}Li plateau.

Keywords. hydrodynamics, convection, radiative transfer, line: profiles, stars: atmospheres, stars: abundances, stars: individual (G020-024, G271-162, HD 74000, HD 84937)

1. Introduction

The spectroscopic signature of the presence of ^{6}Li in the atmospheres of metal-poor halo stars is a subtle extra depression in the red wing of the ^{7}Li doublet, which can only be detected in spectra of the highest quality. Based on high-resolution, high signal-to-noise VLT/UVES spectra of 24 bright metal-poor stars, Asplund *et al.* (2006) report the detection of ^{6}Li in nine of these objects. The average ^{6}Li/^{7}Li isotopic ratio in the nine stars in which ^{6}Li has been detected is $q(\mathrm{Li}) \approx 0.04$ and is very similar in each of these stars, defining a ^{6}Li plateau at approximately $\log n(^6\mathrm{Li}) = 0.85$ (on the scale $\log n(\mathrm{H}) = 12$). A convincing theoretical explanation of this new ^{6}Li plateau turned out to be problematic. Even when the depletion of the ^{6}Li isotope during the pre-main-sequence phase would be ignored, the high abundances of ^{6}Li at the lowest metallicities cannot be explained by current models of galactic cosmic-ray production (for a concise review see e.g. Christlieb 2008, and references therein).

A possible solution of the so-called 'second Lithium problem' was suggested by Cayrel *et al.* (2007), who point out that the intrinsic line asymmetry caused by convection in the photospheres of cool stars is almost indistinguishable from the asymmetry produced by a weak ^{6}Li blend on a presumed symmetric ^{7}Li profile. As a consequence, the derived ^{6}Li abundance should be significantly reduced when the intrinsic line asymmetry in properly taken into account. Using 3D non-LTE line formation calculations based on 3D hydro-dynamical model atmospheres computed with the CO^{5}BOLD code (Freytag *et al.* 2002, Wedemeyer *et al.* 2004, see also http://www.astro.uu.se/~bf/co5bold_main.html), we quantify the theoretical effect of the convection-induced line asymmetry on the resulting ^{6}Li abundance as a function of effective temperature, gravity, and metallicity, for a parameter range that covers the stars of the Asplund *et al.* (2006) sample.

2. 3D hydrodynamical simulations and spectrum synthesis

The hydrodynamical atmospheres used in the present study are part of the CIFIST 3D model atmosphere grid, as described by Ludwig *et al.* (2009). They have been obtained from realistic numerical simulations with the CO^5BOLD code which solves the time-dependent equations of compressible hydrodynamics in a constant gravity field together with the equations of non-local, frequency-dependent radiative transfer in a Cartesian box representative of a volume located at the stellar surface. The computational domain is periodic in x and y direction, has open top and bottom boundaries, and is resolved by typically $140 \times 140 \times 150$ grid points. The vertical optical depth of the box varies from $\log \tau_{\rm Ross} \approx -8$ (top) to $\log \tau_{\rm Ross} \approx +8$ (bottom). The selected models cover the stellar parameter range $5900\,{\rm K} < T_{\rm eff} < 6500\,{\rm K}$, $3.5 < \log g < 4.5$, $-3.0 < {\rm [Fe/H]} < -1.0$.

Each of the selected models is represented by about 20 snapshots chosen from the full time sequence of the corresponding simulation. All these representative snapshots are processed by the non-LTE code NLTE3D that solves the statistical equilibrium equations for a 17 level lithium atom with 34 line transitions, fully taking into account the 3D thermal structure of the respective model atmosphere. The photo-ionizing radiation field is computed at 704 frequency points between $\lambda\,925$ and $32\,407$ Å, using the opacity distribution functions of Castelli & Kurucz (2004) to allow for metallicity-dependent line-blanketing, including the $\rm H\,I$–$\rm H^+$ and $\rm H\,I$–$\rm H\,I$ quasi-molecular absorption near $\lambda\,1400$ and 1600 Å, respectively. Collisional ionization by neutral hydrogen via the charge transfer reaction $\rm H(1s) + Li(n\ell) \leftrightarrow Li^+(1s^2) + H^-$ is treated according to Barklem, Belyaev & Asplund (2003). More details are given in Sbordone *et al.* (2009).

Finally, 3D non-LTE synthetic line profiles of the $\rm Li\,I\,\lambda\,6707$ Å feature are computed with the line formation code Linfor3D (`http://www.aip.de/~mst/linfor3D_main.html`), using the departure coefficients $b_i = n_i({\rm NLTE})/n_i({\rm LTE})$ provided by NLTE3D for each level i of the lithium model atom as a function of geometrical position within the 3D model atmospheres. As demonstrated in Fig. 1, 3D non-LTE effects are very important for the metal-poor dwarfs considered here: not only is the 3D LTE equivalent width too large by more than a factor 2, but also is the half-width of the 3D LTE line profile too narrow by about 10%. Moreover, the lithium lines are significantly less asymmetric if the non-LTE effects are taken into account.

3. Method and Results

As outlined above, the $^6{\rm Li}$ abundance is necessarily overestimated if one ignores the intrinsic asymmetry of the $^7{\rm Li}$ line profile. To quantify this error theoretically, we rely only on synthetic spectra. The idea is to represent the observation by the synthetic 3D non-LTE line profile of the $^7{\rm Li}$ line blend. This 3D flux profile is computed with zero $^6{\rm Li}$ content. Except for an optional rotational broadening, the only source of non-thermal line broadening is the 3D hydrodynamical velocity field, which also gives rise to a convective blue-shift and an intrinsic line asymmetry. Next we compute a small grid of 1D LTE synthetic line profiles of the full $^6{\rm Li}/^7{\rm Li}$ blend from a so-called 1D LHD model, a 1D mixing-length model atmosphere that has the same stellar parameters and uses the same microphysics and radiative transfer scheme as the corresponding 3D model. The parameters of the grid are the total $^6{\rm Li}+^7{\rm Li}$ abundance, $A({\rm Li})$, and the $^6{\rm Li}/^7{\rm Li}$ isotopic ratio, $q({\rm Li})$. Microturbulence is fixed at $\xi_{\rm mic} = 1.5$ km/s, $v \sin i$ is identical to the value used in the 3D spectrum synthesis (we tried 0 and 2 km/s). Now the 1D line profiles from the grid are used to fit the 3D profile. Four parameters are varied independently to find the best fit (minimum χ^2): in addition to $A({\rm Li})$ and $q({\rm Li})$, which control line strength and line asymmetry, respectively, we also allow for an extra line broadening characterized
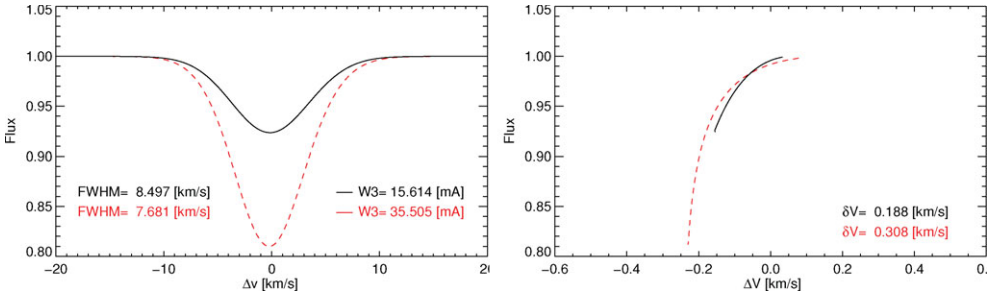
Figure 1. Comparison of 3D LTE (dashed) and 3D non-LTE (solid) line profile (left) and line bisector (right) of a single ^{7}Li component, computed for a typical metal-poor turn-off halo star ($T_{\rm eff}$ = 6300 K, $\log g$ = 4.0, [Fe/H] = -2). Non-LTE effects strongly reduce the equivalent width of the line (W: $35.5 \to 15.6$ mÅ) while they increase the half width of the line profile ($FWHM$: $7.7 \to 8.5$ km/s); the line asymmetry is diminished in non-LTE (velocity span of bisector δv : $0.31 \to 0.19$ km/s).

by $FWHM$ of the Gaussian kernel, and a global line shift, Δv. The value $q^*(\text{Li})$ of the best fit is then identified with the correction $\Delta q(\text{Li})$ that has to be *subtracted* from the $^6\text{Li}/^7\text{Li}$ isotopic ratio determined from the 1D LTE analysis in order to correct for the bias introduced by the intrinsic line asymmetry: $\Delta q(\text{Li}) = q^*(\text{Li})$, and $q^{(3D)}(\text{Li}) = q^{(1D)}(\text{Li})$ - $\Delta q(\text{Li})$. The procedure takes saturation effects properly into account.

We have determined $\Delta q(\text{Li})$ in the relevant range of stellar parameters according to the method outlined above. The results are displayed in Fig. 2 for [Fe/H]=-1 and -2. At given metallicity, the corrections are largest for low gravity and high effective temperature, increasing towards higher metallicity. We note that $\Delta q(\text{Li})$ is essentially insensitive to the choice of $v \sin i$. The downward correction of the $^6\text{Li}/^7\text{Li}$ isotopic ratio is typically in the range $0.01 < \Delta q(\text{Li}) < 0.02$ for the stars of the Asplund *et al.* (2006) sample (see Fig. 2). After subtracting for each of these stars the individual $\Delta q(\text{Li})$, according to $T_{\rm eff}$, $\log g$, and [Fe/H], the mean $^6\text{Li}/^7\text{Li}$ isotopic ratio of the sample is reduced from 0.0212 to 0.0059, as illustrated in Fig. 3. If we keep the error bars given by Asplund *et al.* (2006), the number of stars with a ^{6}Li detection above the 2σ level decreases from 9 to 4. One of them, HD 106038, survives only because of its particularly small error bar of ± 0.006, another one, CD-30 18140, just barely fulfills the 2σ criterion. The remaining two stars are G020-024, which shows the clearest evidence for the presence of ^{6}Li ($q(\text{Li}) = 0.052 \pm 0.017$), and HD 102200 with a somewhat weaker ^{6}Li signal ($q(\text{Li}) = 0.033 \pm 0.013$). The spectra of these stars should be reanalyzed with 3D non-LTE line profiles.
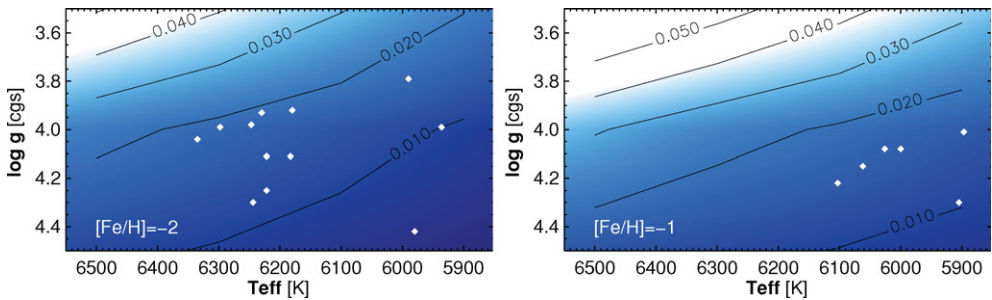

Figure 2. Contours of $\Delta q(\text{Li})$ in the $T_{\rm eff}$ – $\log g$ plane for metallicities [Fe/H]=-2 (left) and [Fe/H]=-1 (right). White symbols mark the positions of the stars from the Asplund *et al.* (2006) sample with $-2.5 <$ [Fe/H] < -1.5 (left), and $-1.5 <$ [Fe/H] < -0.5 (right).
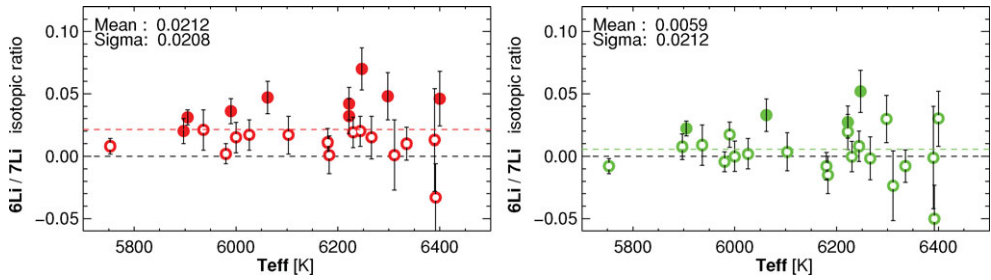
Figure 3. ^{6}Li/^{7}Li isotopic ratio, and $\pm 1\sigma$ error bars, as a function of effective temperature as derived by Asplund *et al.* (2006) before (left) and after (right) subtraction of Δq(Li) to correct for the bias due to the intrinsic line asymmetry. Filled circles denote ^{6}Li detections above the 2σ level, open circles denote non-detections.

Table 1. Fitting three observed Li I $\lambda\,6707$ Å spectra with 1D LTE and 3D non-LTE synthetic line profiles, respectively. Columns (7)–(10) show the results for $v \sin i = 0.0/2.0$ km/s.

Star	T_{eff} [K]	$\log g$	**[Fe/H]**	**S/N**	**Model** [1]	A(**Li**) [2]	q(**Li**) [%]	$FWHM$ [3] [km/s]	Δv [km/s]
HD 74000	6203	4.03	−2.05	600	3D NLTE	2.25/2.25	**−1.1/−1.1**	3.1/2.1	0.64/0.64
					1D LTE	2.23/2.23	**0.6/0.6**	5.9/5.4	0.42/0.42
G271−162	6230	3.93	−2.30	550	3D NLTE	2.30/2.30	**0.6/0.5**	3.6/2.9	0.04/0.05
					1D LTE	2.27/2.27	**2.2/2.2**	6.2/5.7	−0.17/−0.17
HD 84937	6310	4.10	−2.40	630	3D NLTE	2.21/2.20	**4.0/4.2**	3.7/2.7	0.08/0.07
					1D LTE	2.18/2.18	**6.3/6.0**	6.1/5.6	−0.17/-0.14

Notes: [1] $T_{\mathrm{eff}}/\log g/[\mathrm{Fe/H}] = 6280\mathrm{K}/4.0/\text{-}2$; [2] $\log\left[n(^6\mathrm{Li}) + n(^7\mathrm{Li})\right] - \log n(\mathrm{H}) + 12$; [3] Gaussian kernel

As a consistency check, we have also fitted a few observed Li I $\lambda\,6707$ Å spectra with 1D LTE and 3D non-LTE synthetic line profiles, respectively. The fitting parameters are again A(Li), q(Li), $FWHM$, and Δv. As expected, the 3D analysis yields lower q(Li) by roughly -0.02. Details are compiled in Table 1. HD 74000 and G271−162 are considered non-detections, while HD 84937 remains a clear ^{6}Li detection with $q^{(3D)}$(Li) ≈ 0.04.

4. Conclusions

The present study indicates that only 2 or at most 4 out of the 24 stars of the Asplund *et al.* (2006) sample remain significant ^{6}Li detections when subjected to a 3D non-LTE analysis, suggesting that the presence of ^{6}Li in the atmospheres of galactic halo stars is rather the exception than the rule. This would imply that it is no longer necessary to look for a global mechanism accounting for a ^{6}Li enrichment of the galactic halo, but that it is sufficient to explain only a few exceptional cases, which is probably much easier.

References

Asplund, M., Lambert, D. L., Nissen, P. E., Primas, F., & Smith, V. V. 2006, *ApJ*, 644, 229
Barklem, P. S., Belyaev, A. K., Asplund, M. 2003, *A&A*, 409, L1
Castelli, F., & Kurucz, R. L. 2004, arXiv:astro-ph/0405087
Cayrel, R., Steffen, M., Chand, H., Bonifacio, P., Spite, M., Spite, F., Petitjean, P., Ludwig, H.-G., & Caffau, E. 2007, *A&A*, 473, L37
Christlieb, N. 2008, *Journal of Physics G: Nuclear Physics*, 35, 014001
Freytag, B., Steffen, M., & Dorch, B. 2002, *AN*, 323, 213
Ludwig, H.-G., Caffau, E., Steffen, M., Freytag, B., Bonifacio, P., & Kučinskas, A. 2009, *MemSAI*, 80, 708
Sbordone, L., Bonifacio, P., Caffau, E., *et al.* 2009, *A&A* (submitted)
Wedemeyer, S., Freytag, B., Steffen, M., Ludwig, H.-G., & Holweger, H. 2004, *A&A*, 414, 1121